Crystal Structures and ^{35}Cl NQR Spectra of the Metastable and the Stable Phase of Guanidinium bis-Monochloroacetate, $[C(NH_2)_3]^{\oplus}[(ClH_2C)COOH \cdots OOC(CH_2Cl)]^{\ominus}$

Reha Basaran, Shi-qi Dou, and Alarich Weiss

Institut für Physikalische Chemie, Technische Hochschule Darmstadt, Petersenstr. 20, D-6100 Darmstadt, Germany

Z. Naturforsch. **48a**, 478–490 (1993); received January 4, 1993

From acid aqueous solutions of guanidinium carbonate and monochloroacetic acid, $(ClH_2C)COOH:H_2NC(=NH)NH_2 \geqq 2.5$, the compound $[C(NH_2)_3]^{\oplus}[(ClH_2C)COOH \cdots OOC(CH_2Cl)]^{\ominus}$ crystallizes with the space group $C_i^1 - P\bar{1}$, $Z=4$, $a=1147.4$ (5) pm, $b=1113.2$ (5) pm, $c=876.5$ (4) pm, $\alpha=88.66$ (2)°, $\beta=80.31$ (2)°, $\gamma=84.41$ (2)° (metastable phase I). Cooled to 77 K once, phase I transforms at room temperature slowly into the stable phase II, orthorhombic, $D_{2h}^{15} - Pbca$, $Z=8$, $a=1299.2$ (4) pm, $b=1533.7$ (4) pm, $c=1073.9$ (3) pm. The crystal structure determinations show for both phases an ionic lattice with guanidinium cations $[C(NH_2)_3]^{\oplus}$ and acid bis-(monochloroacetate) anions $[(ClH_2C)COOH \cdots OOC(CH_2Cl)]^{\ominus}$ in which a monochloroacetic acid molecule and a monochloroacetate ion are bound to the dimer anion by an asymmetric hydrogen bond $O-H \cdots O$.

A strong crystal field effect, much dependent on temperature, is observed in the ^{35}Cl NQR quadruplet spectrum of phase I, with a frequency spread of ≈ 4 MHz at 300 K, whereas in phase II the frequency splitting of the observed ^{35}Cl NQR doublet is almost constant between 77 K and 310 K, about 700 kHz. The phase transition I → II is very sluggish and unidirectional. The transition II → I needs the recrystallization of II from water.

Structure and dynamics of the two solid phases are discussed.

Introduction

Our interest in the connection between the ^{35}Cl nuclear quadrupole resonance, NQR, spectra of mono-, di-, and trichloroacetates of the general formula $(RNH_3)^{\oplus}((Cl_{3-x}H_xC)COO)^{\ominus}$, $x=0, 1, 2$ [1] led us to investigate also some salts with the anion $((ClF_2C)COO)^-$ [2]. The guanidinium cation $[C(NH_2)_3]^{\oplus}$ was studied in combination with $((ClF_2C)COO)^{\ominus}$ and $((Cl_2HC)COO)^{\ominus}$. It turned out that this cation introduces a strong temperature dependence of the ^{35}Cl NQR spectrum of $((ClF_2C)COO)^{\ominus}$ and $((Cl_2HC)COO)^{\ominus}$. For $[C(NH_2)_3]^{\oplus}((Cl_2HC)COO)^{\ominus}$, $\nu(^{35}Cl)$ of the NQR doublet increases by 2 MHz over the range 77–410 K, and for $[C(NH_2)_3]^{\oplus}$ $((ClF_2C)COO)^{\ominus}$ the singlet frequency $\nu(^{35}Cl)$ decreases by ≈ 5 MHz from 77 K to 275 K, at which temperature a phase transition occurs and $\nu(^{35}Cl)$ is found by 13 MHz lower than above the transition temperature [2]. This anomalous behavior of the salts is most probably connected with the high symmetry of the guanidinium ion. A hydrogen bond network connects the three NH_2 groups of the ion with the carbonyl oxygen atoms, and jumps of the ion around its pseudo-threefold axis or around the pseudo-twofold axes may be the origin of the anomalous temperature behavior and the observed phase transitions.

In course of this work we studied the acid salt guanidinium monochloroacetate, and we report here on the structures and the ^{35}Cl NQR spectra of the two-phase system. A comparison of the structures with the crystal structures (α-phase [3, 4], β-phase [5]) and the ^{35}Cl NQR spectra [6–8] of the three solid phases (α, β, γ) of monochloroacetic acid is also given.

Reprint requests to Prof. Dr. Al. Weiss, Institut für Physikalische Chemie, Technische Hochschule Darmstadt, Petersenstraße 20, W-6100 Darmstadt.

Experimental

The title compound, acid guanidinium monochloroacetate, $[C(NH_2)_3]^{\oplus}[(ClH_2C)COOH \cdots OOC(CH_2Cl)]^{\ominus}$ was prepared from guanidinium carbonate and monochloroacetic acid, both compounds of commercial origin (Aldrich) and used without further purification. The guanidinium carbonate was dissolved in water and $(ClH_2C)COOH$ was added to this solu-

0932-0784 / 93 / 0300-0478 $ 01.30/0. – Please order a reprint rather than making your own copy.

Table 1. Characterization of the guanidinium bis-monochloroacetate, $[C(NH_2)_3]^{\oplus}$ $[(ClH_2C)COOH \cdots OOC(CH_2Cl)]^{\ominus}$; chemical analysis in % weight.

Compound	Habitus	Colour	m.p.[a] [K]	C		H		N	
				Calc.	Found	Calc.	Found	Calc.	Found
$[C(NH_2)_3]^{\oplus}$ $[(ClH_2C)COOH \cdots OOC(CH_2Cl)]^{\ominus}$									
Phase II (stable)	prism	colorless	322	24.21	23.70	4.47	4.46	16.94	16.41
Phase I (metastable)	prism	colorless	322	24.21	23.80	4.47	4.46	16.94	17.45

[a] Decomposition.

tion up to a ratio $((ClH_2C)COOH):[C(NH_2)_3]^{\oplus} = 2.5$. Concentrating the solution at room temperature in air, a colorless crystalline solid precipitates, the crystals being of reasonable size, coarse prisms with edge lengths up to several millimeters. (No effort was made to produce larger size crystals.) The compound was dried in a dessicator over $CaCl_2$. In Table 1 the chemical analysis (C, N, H) and some properties are given.

For the structure determination small single crystals were selected from the material crystallized from solution and later on used for the ^{35}Cl NQR experiments. Since in course of the ^{35}Cl NQR experiments it was found that two solid phases of the compound exist, we mention that small single crystals of phase I (the metastable phase gained from aqueous solution) remain to be single crystals after the thermal treatment which causes the transition to phase II, the stable phase. This is true at least for crystal sizes up to 1 mm^3, and it offers good changes for single crystal NQR work on both phases.

Using a 4-circle X-ray diffractometer (Stoe), diffraction intensities, corrected for absorption and Lorentz-polarization factor, were collected. Therefrom the crystal structures of the two phases of the title compound were determined by direct methods [9]. The hydrogen positions were found from difference Fourier synthesis by a least squares procedure [10]. The thermal amplitudes of the hydrogen atoms were isotropically fixed during the refinement.

The ^{35}Cl NQR spectra have been recorded with a superregenerative spectrometer. For the measurements $\nu(^{35}Cl) = f(\text{temperature } T)$ the wanted temperatures were created at the sample site by a temperature and flow regulated stream of nitrogen gas and by immersing the sample into liquid nitrogen for $T = 77$ K. The sample temperatures have been measured by a thermocouple (copper-constantan) to ± 0.3 K. The width (about 10 kHz) of the NQR lines limits the accuracy of the frequency measurements (± 3 kHz). For comparison, at several temperatures the ^{37}Cl NQR spectrum was observed.

Phase Transition

The relation between phase I and phase II of the title compound was explored qualitatively only. A simple phase indicator is the ^{35}Cl NQR spectrum. Phase I: 4 lines; phase II: 2 lines. Crystallisation from aqueous solution (ratio of cation to acid ≈ 2.5) at room temperature gives phase I. During keeping the compound over $CaCl_2$ in a desiccator at room temperature over weeks, phase I is "stable". Heating up to 300 K has no influence. Cooling down phase I rather quickly (5') to 77 K does not change the ^{35}Cl NQR quadruplet of phase I. When warming up this sample and keeping it at 300 K for several days at this temperature, the two line ^{35}Cl NQR spectrum of phase II is observed, and it does not change over weeks.

If one freezes phase I down to 77 K and measures the ^{35}Cl NQR spectrum from 77 K up, on can observe the spectrum of I for several hours and thereby cover a temperature range from 100 K to 200 K in one experimental run. To complete the spectrum $\nu(^{35}Cl) = f(T)$ of phase I up to 310 K, we started from 200 K up with a fresh sample I. In a further run a sample I was cooled to 253 K (1 h), heated to 288 K (2 h), cooled to 233 K (1.5 h), heated to 288 K (1 h), and cooled to 195 K (3 h). In this experiment, only phase I was detected after each step. We proceeded with this experiment, warming up to 288 K. After several days the spectrum of phase I was weak, and the spectrum of phase II was present with medium intensity. Going down to 220 K (1 h), phase I became weaker, phase II stronger and after 3 more hours phase I was very weak, II strong. Going up to 288 K (2 h), no signal of I, but of phase II only was observable.

Table 2. Experimental conditions for the crystal structure determinations and crystallographic data of guanidinium bis-monochloroacetate. Diffractometer: Stoe-Stadi 4; wavelength: 71.069 pm (MoKα); monochromator: Graphite (002); scan: $2\,\vartheta/\omega$. ϱ_{pyk} was measured at $T = 295$ K.

Compound phase	$[C(NH_2)_3]^{\oplus}$ $[(ClH_2C)COOH \cdots OOC(CH_2Cl)]^{\ominus}$	
	Phase II (stable)	Phase I (metastable)
Formula (molar mass)	$C_5H_{11}Cl_2N_3O_4$ (248.07)	
Crystal size	$(0.35 \times 0.45 \times 0.5)$ mm^3	$(0.25 \times 0.4 \times 2.0)$ mm^3
Temperature/K	299	294
Absorption coefficient (μ/m^{-1})	601.1	585.5
$(\sin\vartheta/\lambda)_{max}$/pm	0.00595	0.00538
Number of measured reflexions	2450	2944
Symmetry independent reflexions	1888	2872
Reflexions considered	1746	2494
Number of free parameters	159	318
F (000)	1024	512
R (F)	0.039	0.045
R_w (F)	0.037	0.040
Lattice constants:		
a/pm	1299.2 (4)	1147.4 (5)
b/pm	1533.7 (4)	1113.2 (5)
c/pm	1073.9 (3)	876.5 (4)
α/°	90.0	88.66 (2)
β/°	90.0	80.31 (2)
γ/°	90.0	84.41 (2)
Volume of the unit cell $V \cdot 10^{-6}$/(pm)^3	2139.83 (3)	1098.29 (4)
Space group	Pbca-D_{2h}^{15}	$P\bar{1}$-c_i^1
Formula units per unit cell	8	4
ϱ_{calc}/Mg · m^{-3}	1.540 (3)	1.500 (4)
ϱ_{pykn}/Mg · m^{-3}	1.52	1.47
Point positions	all atoms in 8c	all atoms in 2i
	x, y, z; $\bar{x}, \bar{y}, \bar{z}$; $\frac{1}{2}+x, \frac{1}{2}-y, \bar{z}$; $\frac{1}{2}-x, \frac{1}{2}+y, z$; $\bar{x}, \frac{1}{2}+y, \frac{1}{2}-z$; $x, \frac{1}{2}-y, \frac{1}{2}+z$; $\frac{1}{2}-x, \bar{y}, \frac{1}{2}+z$; $\frac{1}{2}+x, y, \frac{1}{2}-z$.	x, y, z,; $\bar{x}, \bar{y}, \bar{z}$

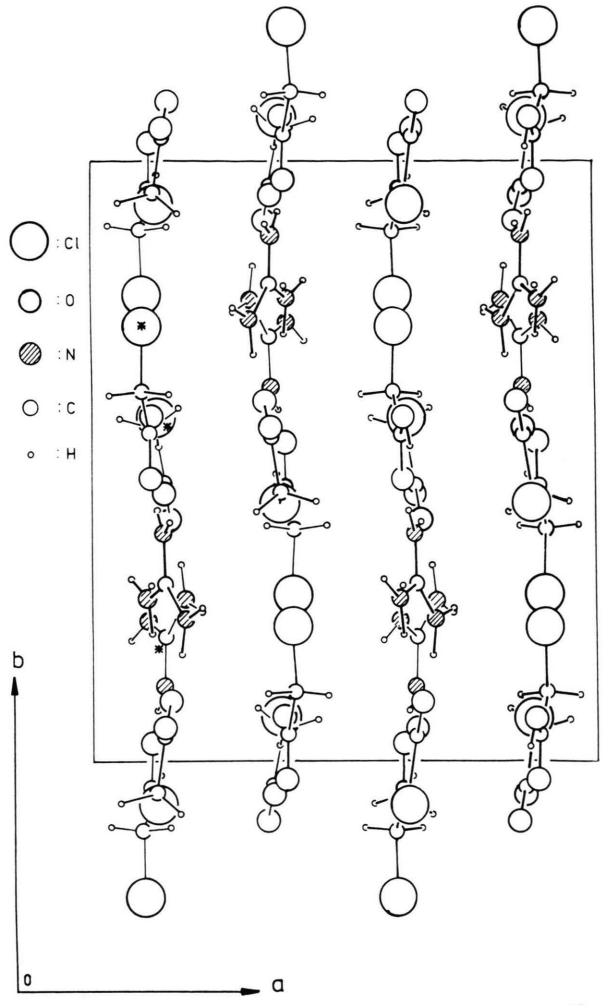

Fig. 1. Projection of the unit cell of $[C(NH_2)_3]^{\oplus}$ $[(ClH_2C)COOH \cdots OOC(CH_2Cl)]^{\ominus}$, stable phase II, along [001] onto the ab plane. Open circles: Large (Cl), medium (O), small (C), very small (H); hatched small circles (N).

We conclude that between 225 K and 190 K the phase transition I → II is initiated (nucleation). The growth of phase II is sluggish, and we have been unable to observe any latent heat by differential thermal analysis. Of the title compound, phase II is the stable and phase I the metastable one.

Results and Discussion

In Table 2 the experimental conditions for the crystal structure determinations are listed, together with some crystallographic data, such as space group, lattice constants, etc., for both solid phases of guanidinium bis-(monochloroacetate).

Crystal Structure of the Stable Phase II and the Metastable Phase I of Guanidinium bis-(Monochloroacetate), $[C(NH_2)_3]^{\oplus}[(ClH_2C)COOH \cdots OOC(CH_2Cl)]^{\ominus}$

The title compound, stable phase II, is available from the metastable phase I by the thermal treatment described above. It crystallizes orthorhombic, space group D_{2h}^{15}-Pbca, with $Z = 8$ chemical units in the

Table 3. Positional and thermal parameters of $[C(NH_2)_3]^{\oplus}$ $[(ClH_2C)COOH \cdots OOC(CH_2Cl)]^{\ominus}$, phase II (stable). The temperature factor is of the form

$$T = \exp\{-2\pi^2 (U_{11}\, h^2 a^{*2} + U_{22}\, k^2 b^{*2} + U_{33}\, l^2 c^{*2} + 2U_{12}\, hk a^* b^* + 2U_{13}\, hl a^* c^* + 2U_{23}\, kl b^* c^*)\}.$$

The U_{ij} are given in $(pm)^2$; U is isotropic mean for the hydrogen atoms.

Atom	x/a	y/b	z/c	U_{11}, U	U_{22}	U_{33}	U_{12}	U_{13}	U_{23}
Cl (1)	0.1011 (1)	0.7232 (0)	0.5554 (1)	859 (4)	412 (4)	672 (5)	16 (3)	−3 (4)	36 (3)
Cl (2)	0.1266 (1)	0.5723 (0)	−0.0646 (1)	1046 (6)	430 (4)	354 (4)	7 (4)	5 (5)	66 (3)
O (1)	0.1159 (1)	0.4692 (1)	0.5533 (2)	724 (12)	389 (10)	461 (11)	0 (9)	−23 (9)	111 (9)
O (2)	0.1221 (1)	0.5699 (1)	0.4032 (2)	829 (13)	410 (11)	291 (9)	−37 (10)	29 (8)	8 (8)
O (3)	0.1423 (1)	0.4444 (1)	0.2499 (2)	944 (14)	418 (10)	264 (9)	3 (9)	−21 (9)	8 (8)
O (4)	0.1543 (1)	0.4011 (1)	0.0540 (1)	825 (13)	341 (9)	320 (9)	23 (9)	14 (8)	−37 (8)
N (1)	0.1827 (2)	0.2652 (2)	0.3349 (2)	791 (17)	447 (14)	418 (14)	−51 (12)	−150 (11)	−13 (11)
N (2)	0.1091 (2)	0.2316 (2)	0.1493 (2)	1098 (22)	457 (16)	406 (14)	−187 (14)	−265 (13)	9 (12)
N (3)	0.1416 (2)	0.1232 (1)	0.2894 (2)	926 (18)	374 (13)	309 (12)	−24 (12)	−38 (12)	29 (10)
C (1)	0.1446 (2)	0.2058 (2)	0.2577 (2)	545 (15)	405 (14)	308 (12)	−16 (12)	11 (10)	12 (11)
C (2)	0.1134 (2)	0.5447 (2)	0.5180 (2)	431 (14)	453 (15)	344 (13)	−24 (11)	−26 (10)	47 (11)
C (3)	0.0980 (2)	0.6154 (2)	0.6125 (2)	592 (18)	503 (16)	381 (14)	−7 (14)	27 (12)	24 (13)
C (4)	0.1416 (2)	0.4581 (2)	0.1330 (2)	482 (14)	385 (14)	342 (14)	−28 (11)	1 (10)	19 (11)
C (5)	0.1240 (2)	0.5524 (2)	0.0974 (2)	667 (19)	383 (15)	311 (14)	6 (12)	−7 (12)	−9 (11)
H (O2)	0.1320 (19)	0.5237 (16)	0.3541 (25)	600					
H′(N1)	0.2174 (19)	0.2468 (17)	0.3907 (25)	600					
H″(N1)	0.1763 (19)	0.3241 (16)	0.3158 (23)	600					
H′(N2)	0.0759 (21)	0.1999 (17)	0.1123 (25)	600					
H″(N2)	0.1158 (18)	0.2900 (16)	0.1242 (25)	600					
H′(N3)	0.1270 (19)	0.0848 (17)	0.2299 (23)	600					

Atom	x/a	y/b	z/c	U_{11}/U
H″(N3)	0.1522 (20)	0.1060 (16)	0.3623 (25)	600
H′(C3)	0.8480 (19)	0.3895 (16)	0.3265 (24)	600
H″(C3)	0.9662 (19)	0.3907 (16)	0.3502 (23)	600
H′(C5)	0.8281 (19)	0.4127 (16)	0.8711 (24)	600
H″(C5)	0.9458 (19)	0.4302 (15)	0.8829 (22)	600

elementary cell, $a = 1299.2$ (4) pm, $b = 1533.7$ (4) pm, $c = 1073.9$ (3) pm. There is one chemical unit in the asymmetric unit of the elementary cell.

The metastable phase I, grown from acidified aqueous solution, crystallizes triclinic centrosymmetric, space group $C_i^1 - P\bar{1}$, $Z = 4$, $a = 1147.4$ (5) pm, $b = 1113.2$ (5) pm, $c = 876.5$ (4) pm, $\alpha = 88.66$ (2)°, $\beta = 80.31$ (2)°, $\gamma = 84.41$ (2)°. Since $Z = 4$, there are two chemical units in the asymmetric unit of the elementary cell. In the following we call the two crystallographically independent units of phase I A and B. The density of metastable phase I is about 2% lower than that of the stable phase II.

In Table 3 positional and thermal parameters of the atoms in phase II are given, and in Table 4 the corresponding data for phase I. For the structure factors F_c, F_o see [17]. Table 5 lists the intra- and intermolecular (ionic) distances and angles for both phases.

In Fig. 1 the unit cell of phase II is shown in projection along the axis [001] onto the *ab* plane. Figure 2 gives the projection of the unit cell of phase I along [100] onto the *bc* plane. In this projection the axis [010] is inclined 5.4° against [001]; [100] is inclined by −9.6° against [001]. A comparison of the projections immediately points out the close relationship between the structures of the phases. From Fig. 1 one recognizes that the ions $[C(NH_2)_3]^{\oplus}$ and $[(ClH_2C)COOH \cdots OOC(CH_2Cl)]^{\ominus}$ are located at *bc* planes centered at $x \approx 1/8$, 3/8, 5/8, and 7/8, and there is no hydrogen bond observed between these layers. The contact is a pure van der Waals-type one. In Fig. 2 we also recognize immediately planes, formed by the cations and anions, parallel to (011). Also here van der Waals contacts only connect these planes in the direction [011].

Not only with respect to very similar layer structures, the layers formed by cations $[C(NH_2)_3]^{\oplus}$ and anions $[(ClH_2C)COOH \cdots OOC(CH_2Cl)]^{\ominus}$, the structures of the two phases are quite closely related. Figures 3 a, b illustrate the structure of phase II by projection of half of the unit cell along [100], Fig. 3 a: $0 \leqq x \leqq 0.5$; Fig. 3 b: $0 \leqq x \leqq 0.25$. In Fig. 3 a the layers centered at $x = 1/8$ and $x = 3/8$ are projected together along [100] onto the (*bc*) plane. In Fig. 3 b a single layer, centered at $x = 1/8$ is shown. All the characteristics of the structure can be seen.

Table 4. Positional and thermal parameters of $[C(NH_2)_3]^{\oplus}$ $[(ClH_2C)COOH \cdots OOC(CH_2Cl)]^{\ominus}$, phase I (metastable). For the definition of the temperature factor see Table 3.

Atom	x/a	y/b	z/c	U_{11}, U	U_{22}	U_{33}	U_{12}	U_{13}	U_{23}
Molecule A									
Cl (1)	1.2211 (1)	0.1219 (1)	0.6623 (1)	632 (6)	987 (8)	1208 (9)	−125 (6)	360 (6)	232 (7)
Cl (2)	0.4958 (2)	0.1921 (2)	0.6325 (2)	515 (8)	1263 (21)	1298 (19)	−67 (12)	−126 (12)	716 (14)
Cl (2a)	0.5074 (9)	0.1406 (8)	0.5508 (11)	815 (53)	808 (54)	1505 (87)	−252 (42)	−623 (62)	374 (47)
O (1)	1.0594 (2)	0.2988 (2)	0.5133 (3)	640 (16)	607 (16)	993 (19)	−169 (13)	−103 (14)	251 (14)
O (2)	0.9134 (2)	0.1785 (2)	0.5365 (3)	554 (16)	671 (17)	1265 (24)	−127 (14)	−318 (16)	296 (16)
O (3)	0.7753 (2)	0.3214 (2)	0.4067 (3)	521 (15)	778 (18)	1033 (20)	−78 (13)	−145 (14)	318 (15)
O (4)	0.5858 (2)	0.3644 (2)	0.3871 (3)	574 (15)	774 (17)	900 (18)	−30 (13)	−236 (13)	288 (14)
N (1)	0.3801 (3)	0.5146 (3)	0.2623 (4)	520 (18)	757 (22)	942 (25)	−113 (18)	−223 (19)	309 (18)
N (2)	0.3221 (3)	0.3648 (3)	0.4310 (4)	580 (21)	748 (22)	958 (25)	−104 (18)	−306 (20)	335 (18)
N (3)	0.1857 (3)	0.4771 (3)	0.3133 (4)	537 (20)	756 (23)	1029 (26)	−160 (17)	−312 (18)	431 (18)
C (1)	0.2960 (3)	0.4526 (3)	0.3356 (4)	610 (23)	529 (21)	674 (23)	−57 (19)	−210 (19)	90 (18)
C (2)	1.0173 (3)	0.2075 (3)	0.5558 (4)	510 (22)	560 (23)	675 (23)	−11 (18)	−63 (18)	46 (18)
C (3)	1.0744 (3)	0.1072 (4)	0.6429 (5)	535 (23)	718 (26)	1043 (34)	−152 (22)	−186 (22)	261 (25)
C (4)	0.6671 (3)	0.3040 (3)	0.4377 (4)	616 (23)	600 (23)	666 (23)	−51 (19)	−132 (20)	82 (18)
C (5)	0.6440 (3)	0.1971 (4)	0.5446 (5)	596 (24)	755 (27)	966 (34)	−114 (21)	−197 (22)	283 (25)
H (O2)	0.8726 (38)	0.2354 (40)	0.4789 (50)	600					
H′(N1)	0.4479 (24)	0.5006 (27)	0.2758 (34)	600					
H″(N1)	0.3686 (24)	0.5741 (26)	0.1965 (33)	600					
H′(N2)	0.2672 (24)	0.3219 (27)	0.4784 (34)	600					
H″(N2)	0.3909 (24)	0.3530 (28)	0.4383 (36)	600					
H′(N3)	0.1291 (25)	0.4317 (25)	0.3624 (32)	600					
H″(N3)	0.1677 (25)	0.5371 (25)	0.2545 (32)	600					
H′(C3)	1.0726 (26)	0.0329 (26)	0.6013 (34)	600					
H″(C3)	1.0283 (24)	0.0924 (26)	0.7421 (31)	600					
H′(C5)	0.6523 (25)	0.1186 (26)	0.4797 (32)	600					
H″(C5)	0.6811 (25)	0.1991 (27)	0.6253 (33)	600					
Molecule B									
Cl (1)	0.7703 (1)	0.8923 (1)	−0.2087 (1)	619 (6)	1282 (10)	1129 (9)	−115 (6)	−124 (6)	203 (7)
Cl (2)	0.0303 (1)	0.8511 (1)	−0.1043 (1)	731 (7)	1014 (8)	1315 (9)	−223 (6)	−425 (7)	640 (7)
O (1)	0.6036 (2)	0.7307 (2)	−0.0316 (3)	766 (18)	884 (20)	950 (20)	−125 (15)	−178 (15)	263 (16)
O (2)	0.4411 (2)	0.8426 (2)	−0.0705 (4)	551 (17)	890 (20)	1458 (27)	−86 (15)	−175 (17)	467 (19)
O (3)	0.2967 (2)	0.7105 (2)	0.0829 (3)	607 (16)	824 (18)	970 (19)	−127 (14)	−286 (15)	343 (15)
O (4)	0.1084 (2)	0.6687 (2)	0.1131 (3)	605 (15)	716 (16)	820 (17)	−173 (13)	−169 (13)	339 (14)
N (1)	0.8889 (3)	0.5057 (3)	0.2251 (4)	611 (22)	970 (27)	1064 (27)	−262 (21)	−331 (22)	360 (21)
N (2)	0.8552 (3)	0.6479 (3)	0.0444 (4)	692 (24)	827 (25)	946 (26)	−227 (20)	−168 (21)	291 (20)
N (3)	0.7069 (3)	0.5380 (3)	0.1589 (4)	549 (22)	882 (26)	938 (26)	−84 (18)	−141 (18)	406 (19)
C (1)	0.8166 (3)	0.5650 (3)	0.1438 (4)	624 (24)	574 (22)	679 (24)	−100 (19)	−83 (20)	62 (19)
C (2)	0.5550 (3)	0.8157 (3)	−0.0876 (4)	674 (26)	638 (25)	780 (26)	−2 (21)	−152 (22)	48 (21)
C (3)	0.6170 (4)	0.9072 (4)	−0.1907 (6)	622 (26)	841 (29)	1215 (40)	9 (23)	−132 (27)	328 (32)
C (4)	0.1907 (3)	0.7274 (3)	0.0563 (4)	658 (24)	570 (22)	618 (23)	−42 (20)	−157 (20)	106 (18)
C (5)	0.1730 (3)	0.8313 (4)	−0.0546 (5)	608 (24)	772 (28)	878 (30)	−153 (22)	−260 (21)	260 (24)
H (O2)	0.3897 (19)	0.7878 (16)	0.0092 (25)	600					
H′(N1)	0.9516 (35)	0.5239 (17)	0.2200 (25)	600					
H″(N1)	0.8578 (36)	0.4468 (17)	0.2958 (26)	600					
H′(N2)	0.8074 (35)	0.6921 (16)	−0.0059 (26)	600					
H″(N2)	0.9251 (37)	0.6667 (17)	0.0416 (27)	600					
H′(N3)	0.6600 (34)	0.5761 (16)	0.1219 (25)	600					
H″(N3)	0.6767 (37)	0.4768 (18)	0.2303 (27)	600					
H′(C3)	0.5932 (34)	0.9118 (16)	−0.2797 (25)	600					
H″(C3)	0.5847 (34)	0.9921 (16)	−0.1613 (25)	600					
H′(C5)	0.2291 (34)	0.8177 (16)	−0.1489 (25)	600					
H″(C5)	0.1855 (34)	0.9026 (16)	−0.0061 (25)	600					

From Figs. 3a, b one finds out that each ion $[C(NH_2)_3]^{\oplus}$ forms 4 hydrogen bonds. One of the three NH_2 groups ($N(3)H_2$) forms two hydrogen bonds: $N(3)H'' \cdots (O(4))$, where O(4) is one of the oxygen atoms of the $OOC(CH_2Cl)$ group of the anion $[(ClH_2C)COOH \cdots OOC(CH_2Cl)]^{\ominus}$ and $N(3)H' \cdots O(1)$, connecting the guanidinium ion via hydrogen bond with the group $(ClH_2C)COOH$ of the anion. The oxygen atom O(4) accepts a second hydrogen bond from N(2), $N(2)H'' \cdots O(4)$. The other hydrogen

Table 5. Selected intra- and intermolecular (interionic) distances (in pm) and intra- and intermolecular (interionic) angles (in degree) of $[C(NH_2)_3]^{\oplus}$ $[(ClH_2C)COOH \cdots OOC(CH_2Cl)]^{\ominus}$. A and B are the crystallographically independent units in the asymmetric unit.

Atoms	Distance			Atoms	Angle		
	Stable phase	Metastable phase			Stable phase	Metastable phase	
		A	B			A	B
Intramolecular:							
Cl (1)–C (3)	176.3 (3)	174.4 (4)	173.1 (4)	Cl (1)–C (3)–H′ C3)	107.1 (15)	107.3 (19)	112.5 (23)
Cl (2)–C (5)	176.6 (3)	175.0 (4)	175.7 (4)	Cl (1)–C (3)–H″ (C3)	105.4 (16)	110.0 (18)	110.2 (27)
O (1)–C (2)	121.9 (3)	119.3 (4)	118.9 (4)	H′(C3)–C (3)–H″(C3)	110.6 (21)	97.4 (26)	93.8 (26)
O (2)–C (2)	129.7 (3)	130.4 (4)	129.7 (4)	Cl (1)–C (3)–C (2)	116.1 (2)	115.2 (3)	115.1 (3)
O (3)–C (4)	127.2 (3)	125.8 (4)	127.1 (4)	Cl (2)–C (5)–H′(C5)	105.0 (17)	97.8 (18)	107.6 (17)
O (4)–C (4)	123.1 (3)	123.5 (3)	123.0 (4)	Cl (2)–C (5)–H″(C5)	100.7 (15)	102.5 (19)	107.7 (19)
O (2)–H (O2)	89.3 (25)	94.0 (42)	105.8 (35)	H′(C5)–C (5)–H″(C5)	114.0 (22)	120.0 (26)	110.8 (27)
C (2)–C (3)	149.9 (3)	149.8 (5)	149.8 (5)	Cl (2)–C (5)–C (4)	114.3 (2)	114.9 (4)	114.2 (3)
C (4)–C (5)	151.3 (3)	151.3 (5)	151.4 (5)	C (2)–O (2)–H (O2)	109.7 (17)	113.9 (28)	115.3 (27)
H′(C3)–C (3)	96.3 (24)	91.5 (28)	86.7 (27)	O (1)–C (2)–O (2)	125.2 (2)	126.1 (3)	125.5 (4)
H″(C3)–C (3)	93.0 (24)	95.8 (26)	100.4 (27)	O (1)–C (2)–C (3)	118.7 (2)	125.6 (3)	124.8 (4)
H′(C5)–C (5)	88.8 (24)	104.2 (27)	96.4 (27)	O (2)–C (2)–C (3)	116.0 (2)	108.3 (3)	109.7 (3)
H″(C5)–C (5)	96.9 (24)	88.7 (26)	94.3 (27)	O (3)–C (4)–O (4)	124.2 (2)	125.4 (3)	125.6 (3)
N (1)–C (1)	132.8 (3)	131.1 (4)	130.4 (4)	O (3)–C (4)–C (5)	114.1 (2)	113.0 (3)	112.9 (3)
N (2)–C (1)	131.3 (3)	131.7 (4)	131.2 (4)	O (4)–C (4)–C (5)	121.7 (2)	121.6 (3)	121.5 (3)
N (3)–C (1)	131.2 (3)	131.4 (4)	130.7 (4)	N (1)–C (1)–N (2)	118.5 (2)	120.0 (3)	120.0 (3)
N (1)–H′(N1)	80.1 (25)	80.6 (26)	76.0 (27)	N (1)–C (1)–N (3)	120.7 (2)	120.3 (3)	119.4 (3)
N (1)–H″(N1)	93.1 (24)	88.3 (27)	94.6 (27)	N (2)–C (1)–N (3)	120.8 (2)	119.7 (3)	120.6 (3)
N (2)–H′(N2)	76.3 (25)	87.2 (27)	87.0 (26)				
N (2)–H″(N2)	93.9 (24)	80.1 (27)	84.4 (27)				
N (3)–H′(N3)	88.9 (25)	90.7 (27)	76.3 (27)				
N (3)–H″(N3)	83.8 (25)	86.4 (27)	96.4 (27)				
Intermolecular:							
O (1) ··· N (2)	324.9 (4)[1]	313.4 (5)[2]	311.9 (4)	N (2)–H′(N2) ··· O (1)	159.4 (18)	143.5 (20)	142.6 (22)
O (1) ··· N (3)	292.3 (4)[1]	294.2 (4)[2]	296.5 (4)	N (3)–H′(N3) ··· O (1)	128.5 (19)	156.5 (21)	151.7 (21)
O (3) ··· N (1)	294.4 (3)	284.9 (3)[a]	284.3 (4)[b]	N (1)–H″(N1) ··· O (3)	168.9 (22)	167.1 (20)	163.6 (21)
O (3) ··· O (2)	254.7 (2)	252.3 (4)	252.0 (4)	O (2)–H (O2) ··· O (3)	173.3 (19)	165.9 (19)	163.1 (20)
O (4) ··· N (1)	348.8 (3)[3]	309.4 (4)	325.1 (4)[4]	N (1)–H′(N1) ··· O (4)	123.5 (18)	145.8 (20)	148.8 (21)
O (4) ··· N (2)	285.4 (2)	298.4 (4)	309..6 (4)[4]	N (2)–H″(N2) ··· O (4)	162.1 (18)	159.4 (21)	158.3 (21)
O (4) ··· N (3)	287.0 (3)[3]	301.1 (4)[a]	289.8 (4)[b]	N (3)–H″(N2) ··· O (4)	167.9 (19)	170.0 (21)	174.3 (21)
O (1) ··· H′(N2)	271.9 (24)[1]	239.0 (24)[2]	238.3 (25)				
O (1) ··· H′(N3)	207.4 (23)[1]	208.8 (25)[2]	227.1 (26)				
O (3) ··· H″(N1)	202.5 (24)	191.9 (26)[a]	198.5 (26)[b]				
O (3) ··· H (O2)	165.8 (26)	160.1 (25)	148.9 (25)				
O (4) ··· H′(N1)	298.1 (25)[3]	239.4 (25)	257.7 (26)[4]				
O (4) ··· H″(N2)	192.9 (24)	222.1 (26)	229.6 (26)[4]				
O (4) ··· H″(N3)	206.1 (24)[3]	205.7 (25)[a]	203.7 (26)[b]				
Cl (1) ··· Cl (2)[c]	340.7 (3)[5]	328.7 (4)[11]	325.3 (4)[11]				
Cl (1) ··· N (2)	350.8 (3)[6, 7]	351.1 (4)[c, 11]	363.3 (4)[c, 11]				
Cl (2) ··· N (2)[c]	—	332.7 (4)	327.4 (5)[11]				
Cl (1) ··· N (1)	370.3 (3)[7]	—	—				
Cl (1) ··· N (2)	—	361.3 (4)[a, 12]	382.9 (5)[b, 13]				
Cl (1) ··· O (1)	—	—	362.9 (4)[b, 13]				
Cl (1) ··· O (4)	370.6 (3)[8]	—	—				
Cl (2) ··· N (3)	—	390.4 (4)[a, 14]	—				
Cl (2) ··· O (1)	363.3 (3)[8]	358.9 (4)[a, 14]	—				
Cl (2) ··· O (2)	394.2 (3)[9]	402.8 (4)[a, 14]	375.1 (4)[b, 13]				
Cl (2) ··· O (3)	361.2 (3)[10]	396.2 (4)[a, 14]	362.0 (4)[b, 13]				

[1] O (1):	x,	$\frac{1}{2}-y$,	$-\frac{1}{2}+z$
[2] O (1):	$-1+x$,	y,	z
[3] O (4):	x,	$\frac{1}{2}-y$,	$\frac{1}{2}+z$
[4] O (4):	$1+x$,	y,	z
[5] Cl (1):	x,	$\frac{3}{2}-y$,	z
[6] Cl (1):	$\frac{1}{2}+x$,	y,	$\frac{1}{2}-z$
[7] N (1), N (2):	$\frac{1}{2}-x$,	$\frac{1}{2}+y$,	z
[8] O (1), O (4):	$\frac{1}{2}-x$,	$1-y$,	$\frac{1}{2}+z$
[9] O (2):	$\frac{1}{2}-x$,	$1-y$,	$-\frac{1}{2}+z$
[10] O (3):	$\frac{1}{2}-x$,	$1-y$,	$\bar{z}$
[11] $Cl(1)_A$, $Cl(1)_B$, $N(2)_B$:	$1-x$,	y,	z
[12] $Cl(1)_A$:	$2-x$,	$1-y$,	$1-z$
[13] $Cl(1)_B$, $Cl(2)_B$:	$1-x$,	$1-y$,	$1-z$
[14] $Cl(2)_A$:	$1-x$,	$1-y$,	$-z$

[a] Mol. A ··· Mol. B; [b] Mol. B ··· Mol. A; no letter: Mol. A ··· Mol. A, Mol. B ··· Mol. B; [c] The van der Waals distances within the layer; all other distances are between two layers.

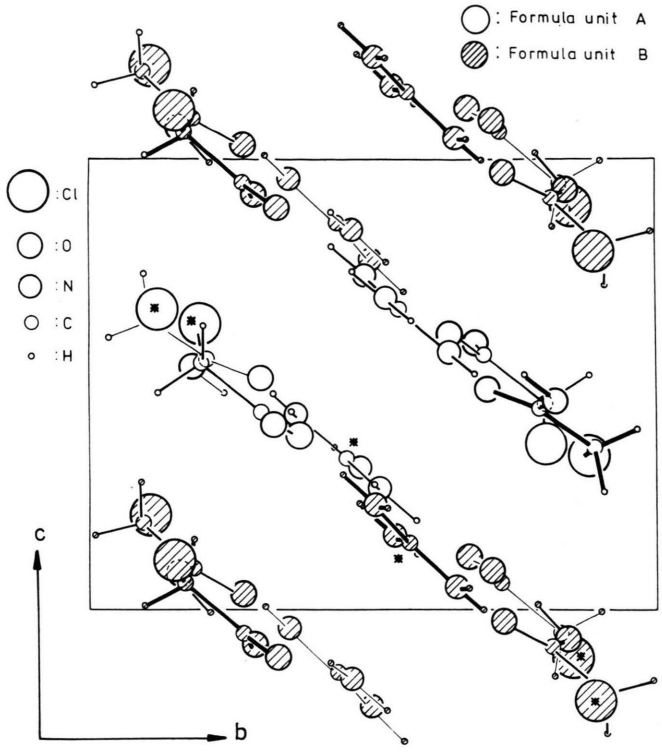

Fig. 2. Projection of the unit cell of phase I (metastable) of $[C(NH_2)_3]^{\oplus}[(ClH_2C)COOH \cdots OOC(CH_2Cl)]^{\ominus}$ along [100] onto the *bc* plane. Open circles mark cation and anion A of the asymmetric unit, hatched symbols mark cation and anion B. The stared ions are the ones for which the coordinates are given Table 4.

of the group $N(2)H_2$ is not involved in a hydrogen bond. The third NH_2 group of the guanidinium ion, $N(1)H_2$, forms, as $N(2)H_2$, only one bond, $N(1)H'' \cdots O(3)$. Looking on the anion $[(ClH_2C)COOH \cdots OOC(CH_2Cl)]^{\ominus}$, the hydrogen of the carboxyl group C(2)O(1)O(2)H(O2) forms a hydrogen bond $O(2)-H(O2) \cdots O(3)$. O(2) is the only oxygen atom of the anion not connected by bonds $N-H \cdots O$ to the guanidinium ion. The single plane projection given in Fig. 3b points out that the *bc* planes are in reality ribbons built by hydrogen bonds between the anions and cations, running along the *c* direction. By van der Waals interactions $Cl \cdots Cl$ planes are formed. Figures 3a, b show also that there is no hydrogen bond connection in the direction [100] between the layers parallel to the *bc* plane.

Quite similar is the layer structure of phase I. In Figs. 4a, b we show the projections of part of the unit cell along [001]. The first layer (the stared one in Fig. 2) is shown in Figure 4a. It is pointed out that there are two units $[C(NH_2)_3]^{\oplus}[(ClH_2C)COOH \cdots OOC(CH_2Cl)]^{\ominus}$ in the asymmetric unit, unit A (open circles in Figs. 2, 4a, and 4b). The hatched symbols stand for unit B. In the Figs. 4a, b the hydrogen bonded anion $[(ClH_2C)COOH \cdots OOC(CH_2Cl)]^{\ominus}$ is clearly seen. The guanidinium ion A is connected via hydrogen bonds with the anion A and B, and the cation B with the anions A and B.

For ease of discussion, we have used the same numbering for "chemical bond equivalent" atoms in phase II and phase I, unit A and unit B, troughout the paper, see Tables 3, 4, 5 etc. and the figures.

Considering bond lengths and bond angles, see Table 5, the bond lengths C–N in the guanidinium ion are quite regular. For phase II one finds $131.2 \leqq d(C-N)/pm \leqq 132.8$; $\langle d(C-N)\rangle = 131.8$ pm. For phase I $130.7 \leqq d(C-N)/pm \leqq 131.7$; $\langle d(C-N)\rangle =$ 131.1 pm (both units A and B). This regularity is also observed for the angles $(N-C-N) \leqq 120.8°$; $\langle°\rangle =$ 120.0°; phase I: $119.4 \leqq \langle(N-C-N)/° \leqq 120.6$; $\langle°\rangle =$ 120.0°. One concludes that the CN_3 frame of the ion $[C(NH_2)_3]^{\oplus}$ is, within the limits of error, planar, as reported in [2]. We have calculated the best planes trough the atoms C, N(1), N(2), and N(3) of the guanidinium ions. They are given by (*d* in Å) by

$$a x + b y + c z = d. \qquad (1)$$

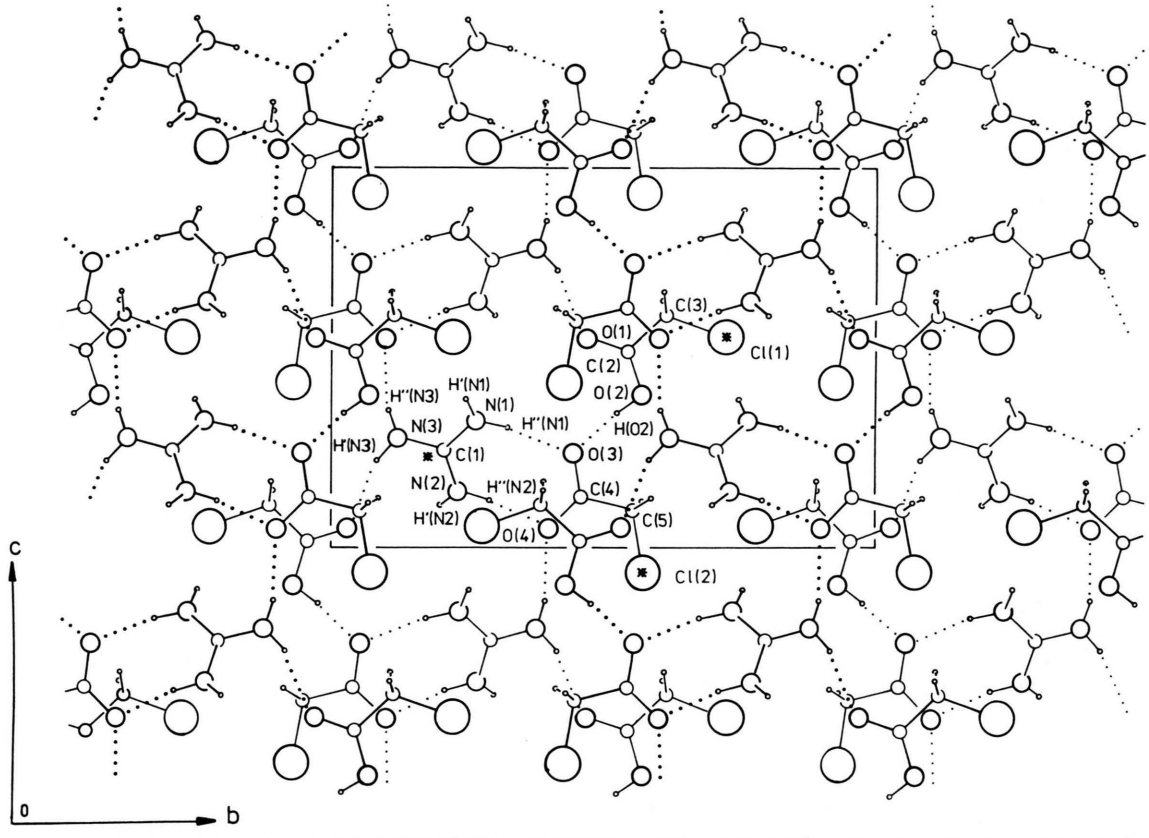

Fig. 3a. Projection of the unit cell of $[C(NH_2)_3]^{\oplus}$ $[(ClH_2C)COOH \cdots OOC(CH_2Cl)]^{\ominus}$, stable phase II, along [100], from $x=0$ to $x=0.5$, onto the bc plane. The hydrogen bonds are marked by dotted lines.

The results are:

Phase II $\quad 11.7785\,x-2.0300\,y-4.3032\,z=0.1734.$

Phase I, A $\quad 0.3215\,x+7.3027\,y+6.5951\,z=5.6110;$

B $\quad -0.8846\,x+7.5815\,y+6.1313\,z=4.4316.$

The deviations of the carbon and the nitrogen atoms from the best planes are within the limits of error (maximum for phase II: 0.3 pm; maximum for phase I, A: 0.3 pm, B: 1.1 pm. In the three crystallographically different ions the carbon atoms is at the top of very flat trigonal pyramids, as one would guess).

The structure of the anion $[(ClH_2C)COOH \cdots OOC(CH_2Cl)]^{\ominus}$ is determined by the asymmetric position of the hydrogen atom H(O2) which is bound to O(2) and forms a hydrogen bond to O(3). The bond lengths within th groups COOH and COO of the anion are of interest. We observe a small difference between $d(C(2)-C(3)) = 149.8$ pm and $d(C(4)-C(5)) = 151.4$ pm for phase I and phase II, both well in the range observed for aliphatic C–C distances. The distances C–O within the carboxyl group differ considerably, from 122 pm for C(2)–O(1) to 130 pm for C(2)–O(2) in the group COOH, and from 123 pm for C(4)–O(4) to 127 pm for C(4)–O(3) in the group COO of phase II (in phase I: 119 pm ... 130 pm and 123 pm ... 127 pm, respectively). We have calculated the best planes trough the carbon and oxygen atoms of the anions $[(ClH_2C)COOH \cdots OOC(CH_2Cl)]^{\ominus}$, separately for the groups C(2) C(3) O(1) O(2) and C(4) C(5) O(3) O(4). The hydrogen H(O2) was not included in the calculation. With (1) it was found

[C(2) C(3) O(1) O(2)]	[C(4) C(5) O(3) O(4)]
Phase II	
$12.8717\,x+1.0719\,y+1.2502\,z=2.6877$	$12.8153\,x+2.4988\,y+0.2324\,z=2.9917$
Phase I	
A	A
$-2.6820\,x+4.6401\,y+7.1695\,z=2.2216$	$0.8330\,x+6.8394\,y+6.9605\,z=5.6765$
B	B
$2.6427\,x+6.3754\,y+7.2924\,z=6.0274$	$-0.4979\,x+7.0209\,y+6.6179\,z=5.3881$

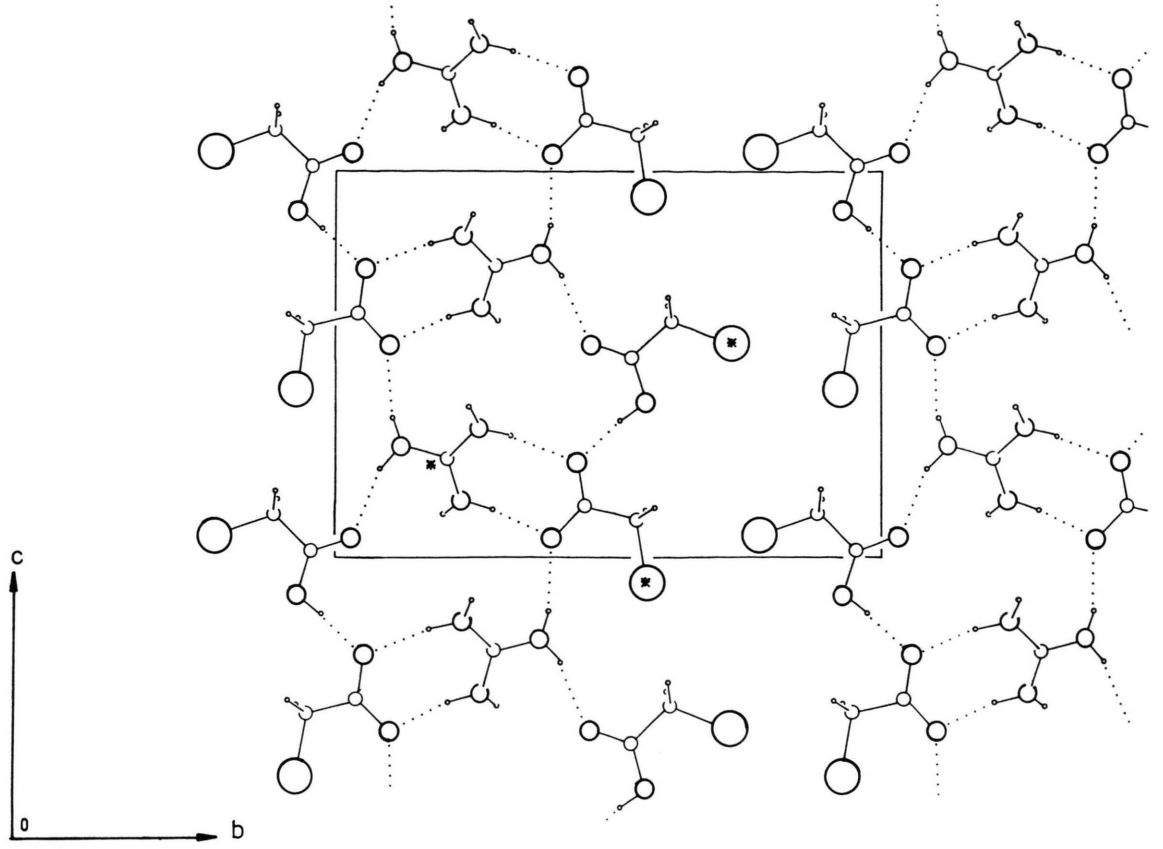

Table 3 b. Projection of the unit cell of $[C(NH_2)_3]^{\oplus}[(ClH_2C)COOH \cdots OOC(CH_2Cl)]^{\ominus}$, stable phase II, along [100], from $x=0$ to $x=0.25$, onto ($b\,c$). The hydrogen bonds are marked by dotted lines.

The deviations of the involved atoms for the best planes are small; in phase II 0.3 pm (the hydrogen of the OH group is 1.5 pm off the plane) and 0.1 pm, respectively; in phase I the deviations of the atomic positions are at most 0.4 pm (3.8 pm for the hydrogen) and 0.5 pm for the anion A, and 0.4 pm (9.5 pm for the hydrogen) and 0.3 pm, respectively, for the anion B. The angles the two planes C(2)C(3)O(1)O(2) and C(4)C(5)O(3)O(4) form are 7.62° in phase II, 20.63° in the anion A and 16.58° in the anion B of phase I.

For the interpretation of the ^{35}Cl NQR results the bond lengths Cl–C have some weight. Within the limits of error, d(Cl(1)–C(3)) and d(Cl(2)–C(5)) are equal, 176.3 pm and 176.6 pm, respectively, for phase II and 173.1 pm ... 175.7 pm for phase I.

^{35}Cl NQR in Phase II and Phase I of $[C(NH_2)_3]^{\oplus}$ $[(ClH_2C)COOH \cdots OOC(CH_2Cl)]^{\ominus}$

The ^{35}Cl NQR spectrum of the stable phase II of the title compound is shown as a function of temperature in Figure 5. It is a doublet, in accordance with the crystal structure. The frequencies decrease with increasing temperature, as one expects from the influence of librational motions on the electric field gradient, EFG, at the chlorine site [11]. In Table 6 the results of the power series expansion of $\nu(^{35}Cl) = f(T)$ are given for phase II and phase I. Table 7 lists the ^{35}Cl NQR frequencies, selected for two temperatures, together with the observed signal to noise ratio, S/N.

Figure 6 presents the ^{35}Cl NQR spectrum of phase I as function of temperature. In accordance with the crystal structure, the spectrum is a quadruplet; the temperature dependence is as expected [11]. The results of the parameterization of $\nu(^{35}Cl) = f(T)$ are

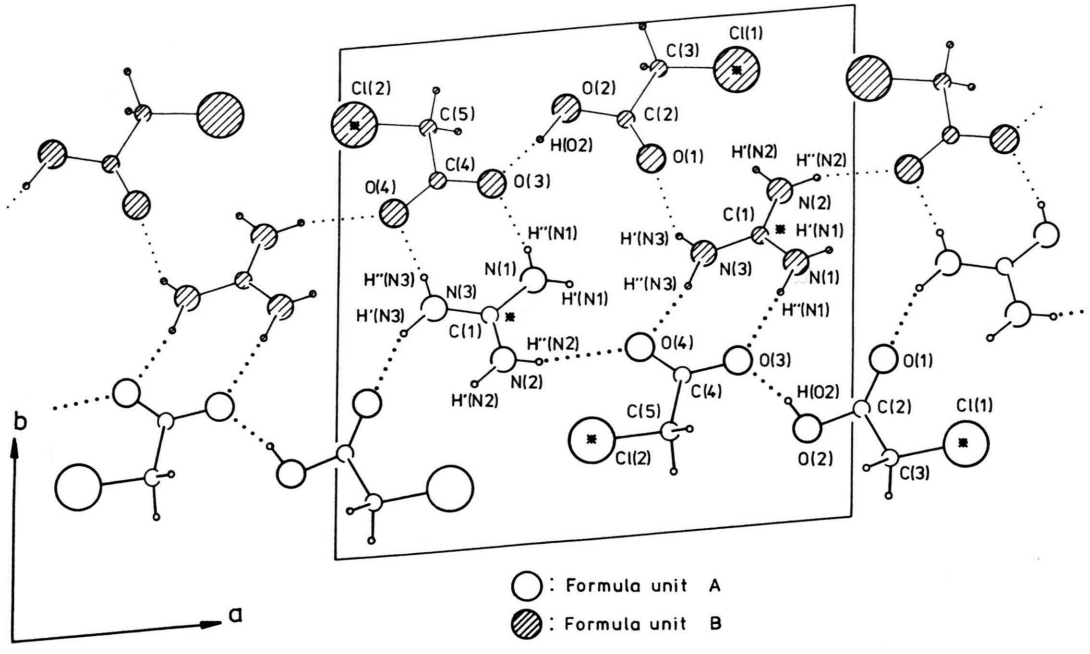

Fig. 4a. Projection of part of the unit cell of phase I of the title compound (first layer) along [001] onto (*a b*). Open circles: Ion pair A; hatched circles: Ion pair B. The hydrogen bonds are marked by dotted lines. The stared ions are the ones for which the coordinates are given in Table 4.

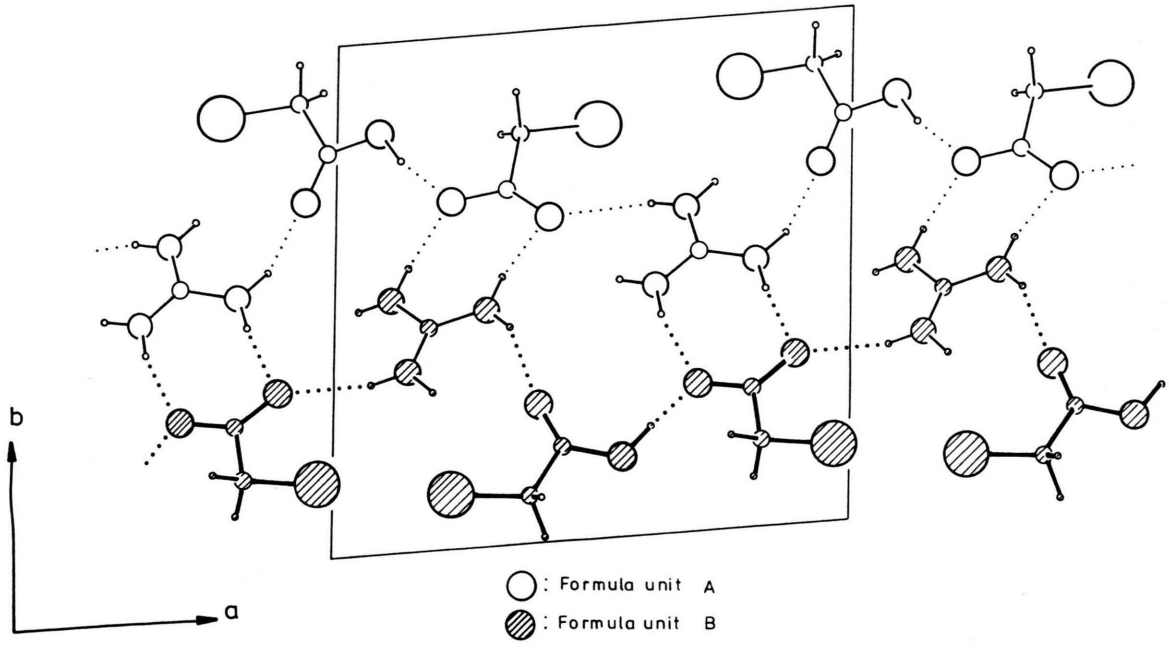

Fig. 4b. As Fig. 4a, but the second layer is projected.

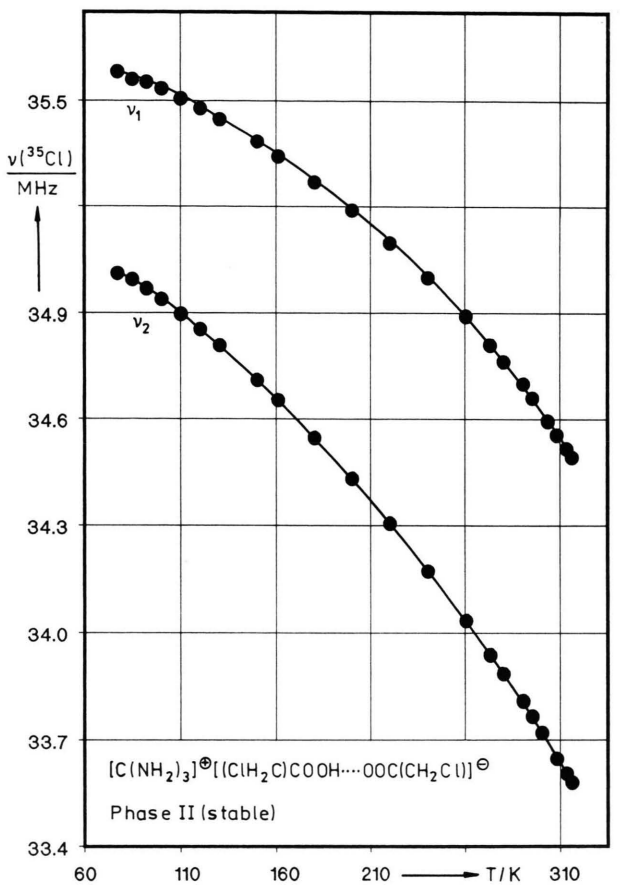

Fig. 5. ^{35}Cl NQR frequencies of phase II (stable) of $[C(NH_2)_3]^{\oplus}[(ClH_2C)COOH \cdots OOC(CH_2Cl)]^{\ominus}$ as function of temperature.

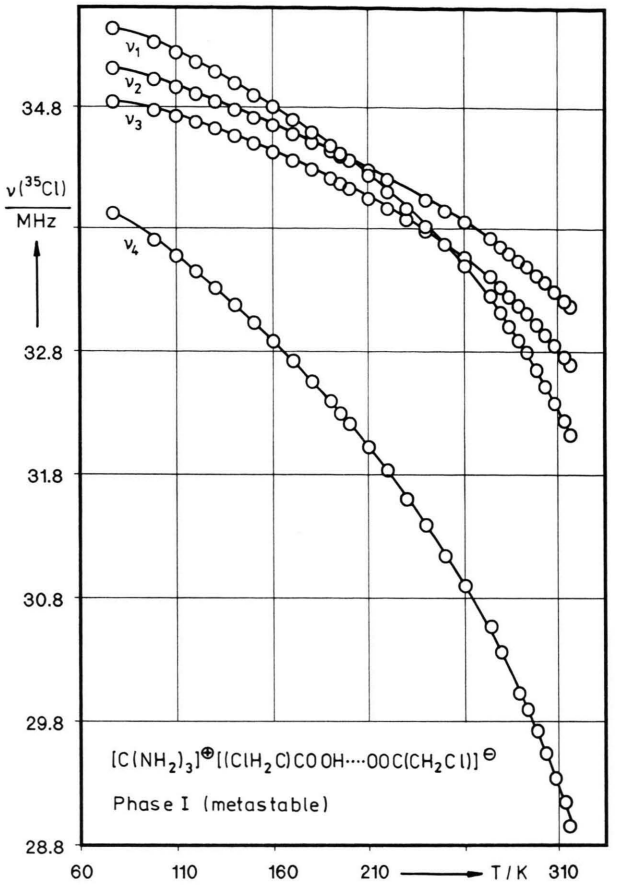

Fig. 6. ^{35}Cl NQR spectrum of phase I (metastable) of $[C(NH_2)_3]^{\oplus}[(ClH_2C)CCOOH \cdots OOCCH_2Cl)]^{\ominus}$ as a function of temperature.

Table 6. Power series expansion of $\nu(^{35}Cl) = f(T)$ for the guanidinium bis-monochloroacetate: $f(T) = \sum_{i=-1}^{3} a_i T^i$; ΔT: Temperature range for which the power series is valid; Z: Number of data; σ: Standard deviation.

Compound	ν_i	ΔT	Z	σ / kHz	a_{-1} / MHz · K	a_0 / MHz	$a_1 \cdot 10^3$ / MHz · K^{-1}	$a_2 \cdot 10^6$ / MHz · K^{-2}	$a_3 \cdot 10^9$ / MHz · K^{-3}
$[C(NH_2)_3]^{\oplus}[(ClH_2C)COOH \cdots OOC(CH_2Cl)]^{\ominus}$									
Phase II	ν_1	77-316.2	22	3.2	−31.014	36.579	−9.694	29.461	−59.110
	ν_2	77-316.2	22	2.5	−29.881	36.026	−9.287	18.016	−38.478
Phase I	ν_1	77-316.6	29	9.0	−136.955	39.741	−43.508	159.435	−295.418
	ν_2	77-316.6	28	3.8	−71.953	37.449	−23.222	73.996	−129.902
	ν_3	77-316.6	29	5.9	−91.398	37.641	−27.373	96.358	−177.955
	ν_4	77-315.6	28	14.7	−114.535	38.040	−43.898	150.277	−309.655

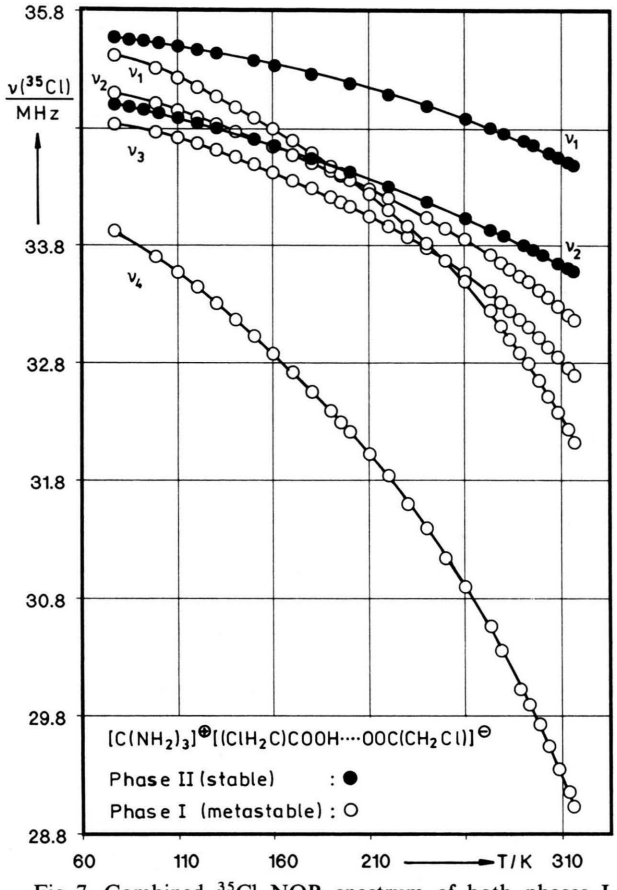

Fig. 7. Combined ^{35}Cl NQR spectrum of both phases I (metastable) and II (stable) of the studied compound, $[C(NH_2)_3]^{\oplus}[(ClH_2C)CCOOH \cdots OOCCH_2Cl)]^{\ominus}$.

listed in Table 6, and in Table 7 selected frequencies are given numerically.

Comparison of Phase I and II, Structure, Dynamics, and ^{35}Cl NQR

The NQR spectra of phase I and phase II are combined in Figure 7. The differences between phases I and II in the temperature dependence of $\nu(^{35}Cl)$ are remarkable. In phase II $\Delta\nu_1(^{35}Cl)/\Delta T$ is about 4 kHz/K, $\Delta\nu_2(^{35}Cl)/\Delta T = 6$ kHz/K. The situation changes drastically when considering phase I. We find $\Delta\nu_1(^{35}Cl)/\Delta T = 15$ kHz/K, $\Delta\nu_2(^{35}Cl)/\Delta T = 8$ kHz/K, $\Delta\nu_3(^{35}Cl)/\Delta T = 9$ kHz/K, and $\Delta\nu_4(^{35}Cl)/\Delta T = 28$ kHz/K (see Figure 6). The conclusion is that librational motions in the lattice of the metastable phase I are excited much more strongly than the ones in the stable phase I.

First we shall discuss the question: Can we assign the two ^{35}Cl NQR frequencies of phase II to Cl(1) and Cl(2) in the unit cell of II and can we correlate $\nu_1(^{35}Cl) \ldots \nu_4(^{35}Cl)$ of phase I with the chlorines $Cl(1)_A$, $Cl(2)_A$, $Cl(1)_B$, and $Cl(2)_B$?

Table 7. ^{35}Cl NQR frequencies of guanidinium bis-monochloroacetate at selected temperatures and signal to noise ratios S/N (lock in technique; time constant 10 s).

Compound	ν_i	$\frac{\nu(^{35}Cl)}{MHz}\left(\frac{T}{K}\right)$	$\frac{S}{N}$	$\frac{\nu(^{35}Cl)}{MHz}\left(\frac{T}{K}\right)$	$\frac{S}{N}$
$[C(NH_2)_3]^{\oplus}[(ClH_2C)COOH \cdots OOC(CH_2Cl)]^{\ominus}$					
Phase II	ν_1	35.582 (77)	35	34.660 (295.4)	12
	ν_2	35.012 (77)	51	33.766 (295.4)	14
Phase I	ν_1	35.429 (77)	27	32.654 (298.2)	7
	ν_2	35.108 (77)	23	33.418 (298.2)	9
	ν_3	34.841 (77)	17	33.019 (298.2)	7
	ν_4	33.926 (77)	15	29.731 (298.2)	5

From proton transfer complexes XY, where Y is trichloroacetic acid and X is a proton acceptor, one has learned that the ^{35}Cl NQR frequencies are shifted downwards, in comparison with the pure trichloroacetic acid, if the proton is transferred to the acceptor, i.e. if we approach the ionic state $Y^{\ominus}$ [12]. For monochloroacetic acid such a behavior was observed, too [13]. Using this finding, we conclude that in the anion $[(ClH_2C)COOH \cdots OOC(CH_2Cl)]^{\ominus}$ of phase II $\nu_1(^{35}Cl)$ is the NQR frequency of Cl(1), the Cl-atom bonded in the group $(ClH_2)COOH$ of the anion, and $\nu_2(^{35}Cl)$ belongs to Cl(2), the chlorine which is part of the group $OOC(CH_2Cl)$.

The assignment $\nu_1(^{35}Cl) \leftrightarrow Cl(j)$ is more difficult (and uncertain) in case of phase I. Firstly we consider $\nu_4(^{35}Cl)$. This is, over the whole temperature range investigated, the lowest frequency. With the rule given above we assign it to a chlorine of the group $(ClH_2)COOH$, either to $Cl(2)_A$ or to $Cl(2)_B$. To do this, we must consider the temperature dependence of $\nu_4(^{35}Cl)$ and the temperature factors of the Cl-atoms of phase I, see Table 4. From Fourier synthesis and least squares refinement of the structure it turned out that $Cl(2)_A$ is in a split position, $Cl(2)_A$ and $Cl(2a)_A$. The ratio of the site occupation factors is $Cl(2)_A : Cl(2a)_A = 0.8 : 0.2$, showing strong librational motions of the group $[(ClH_2C)COO]_A$. We have also a look on the hydrogen bond system in which $[(ClH_2)COO]_A$ and $[(ClH_2)COO]_B$ are involved (see also Table 5 and Figure 4a). The oxygen atoms $O(4)_A$ and $O(3)_A$ are each involved in two hydrogen bonds: $O(3)_A \cdots (H(O2)-O(2))_A$, $O(3)_A \cdots (H''(N1)-(N1))_B$, $O(4)_A \cdots (H''(N2)-N(2))_A$, $O(4)_A \cdots (H''(N3)-N(3))_B$. The corresponding distances are $O(3)_A \cdots O(2)_A =$

252 pm; $O(3)_A \cdots N(1)_B = 285$ pm, $O(4)_A \cdots N(2)_A = 298$ pm, $O(4)_A \cdots N(3)_B = 301$ pm. For comparison we give the corresponding distances of the unit B. $O(3)_B \cdots O(2)_B = 252$ pm, $O(3)_B \cdots N(1)_A = 284$ pm, $O(4)_B \cdots N(2)_B = 304$ pm, $O(4)_B \cdots N(3)_A = 290$ pm. Assuming for the van der Waals radii of NH_2 and Cl 175 pm, for oxygen 1.5 pm [14], the distances discussed are within the limits for hydrogen bond. There is no reason to distinguish between the hydrogen bond scheme of the two groups A and B. Therefore we relay on the X-ray results only in assigning $\nu_4(^{35}Cl) \leftrightarrow Cl(2)_A$.

With this assumption and the comparison of the temperature coefficients of $\nu_{1-3}(^{35}Cl)$ we correlate $\nu_1(^{35}Cl)$ of phase I with $Cl(1)_A$. From the discussion above on the correlation of NQR frequency and ionic charge of the group in question, we find $\nu_2(^{35}Cl) \leftrightarrow Cl(2)_B$ and $\nu_3(^{35}Cl)_I \leftrightarrow Cl(1)_B$.

As mentioned, there exist three solid phases for monochloroacetic acid. The α-phase is the stable one, consisting of tetrameric units and in the asymmetric unit of the unit cell there are two independent molecules [3, 4]. Consequently there are two crystallographically different Cl-atoms with ^{35}Cl NQR frequencies of 34.97 MHz and 35.52 MHz at 292 K [6]. Both frequencies are higher than the ones we observe for phase II of the title compound; this correlates with the fact that there is no strong ionic character in α-$(ClH_2C)COOH$. The β-phase of monochloroacetic acid consists of dimeric units $((ClH_2C)COOH)_2$, an arrangement quite common for carboxylic acids [15]. The ^{35}Cl NQR frequency is found at 35.54 MHz (292 K) and is somewhat higher than the frequencies we observe for the two phases of the title compound. The ^{35}Cl NQR singulet of the γ-phase of $(ClH_2C)COOH$ is found in the same frequency range where the NQR spectrum of the α- and β-phase appears.

From this comparison we find that there is an influence of the ionic part of the crystal field in the title compound $[C(NH_2)_3]^{\oplus}[(ClH_2C)COOH \cdots OOC(CH_2Cl)]^{\ominus}$ which induces an EFG opposite to the one due to the bond C–Cl.

Van der Waals Interactions

An interesting point are the van der Waals interactions in the title compound [16]. The ion pair $[C(NH_2)_3]^{\oplus}[(ClH_2C)COOH \cdots OOC(CH_2Cl)]^{\ominus}$ is found in three different surroundings, differences caused by the packing of the ions in phase II and in the phases I A and I B. Certainly, the main contribution to the crystal field effect is due to the Coulomb field created by the charge distribution in the solids considered. There is, however a fairly large variation in the van der Waals interaction. The van der Waals pairs of interest are $Cl \cdots Cl$, $Cl \cdots H_2N$, and $Cl \cdots O$. In Table 5 the intermolecular (ionic) distances are listed. We find for the two phases of the title compound van der Waals contacts within layer and between the layers. In phase II there is an intralayer contact $Cl \cdots Cl$ of 341 pm and several interlayer contacts $Cl \cdots NH_2$ and $Cl \cdots O$ (351 pm ... 394 pm). In phase I the two intralayer distances d_{vdw} $(Cl \cdots Cl)$ observed are quite short, 329 pm $(A \cdots A)$ and 325 pm $(B \cdots B)$.

Acknowledgement

We are grateful to the Fonds der Chemischen Industrie for support of the work. R. B. is obliged to the Department of Physics of the University of Istanbul for granting leave of absence.

[1] R. Basaran, S.-q. Dou, and Al. Weiss, Ber. Bunsenges. Phys. Chem. **96,** 35 (1992).
[2] R. Basaran, S.-q. Dou, and Al. Weiss, Z. Naturforsch. **47a,** 241 (1992).
[3] B. Kalyanaraman, J. L. Atwood, and L. D. Kispert, J. Chem. Soc. Chem. Comm. **1976,** 715.
[4] J. A. Kanters and G. Roelofsen, Acta Cryst. **B 32,** 3328 (1976).
[5] J. A. Kanters, G. Roelofsen, and T. Feenstra, Acta Crysts. **B 32,** 3331 (1976).
[6] H. Negita, J. Chem. Phys. **23,** 214 (1955).
[7] H. C. Allen Jr., J. Amer. Chem. Soc. **74,** 6074 (1952); Phys. Rev. **87,** 227 (1952); J. Phys. Chem. **57,** 501 (1953).
[8] V. S. Grechishkin, Zh. Fiz. Khim. **35,** 1803 (1961).
[9] G. M. Sheldrick, SHELX 86, Program for Crystal Structure Solution, University of Göttingen, Germany 1986.
[10] G. M. Sheldrick, SHELX 76, Program for Crystal Structure Determination, University of Cambridge, England 1976.
[11] H. Bayer, Z. Phys. **130,** 227 (1951).
[12] D. Biedenkapp and Al. Weiss, Ber. Bunsenges. Phys. Chem. **70,** 788 (1966).
[13] R. J. Lynch, T. C. Waddington, T. A. O'Shea, and J. A. C. Smith, J. Chem. Soc. Faraday II, **72,** 1980 (1976).
[14] A. Bondi, J. Phys. Chem. **68,** 441 (1964); A. Bondi, Physical Properties of Molecular Crystals, Liquids, and Glasses, J. Wiley & Sons, New York 1968.
[15] J. C. Speakman, Structure and Bonding **12,** 141 (1972).
[16] Al. Weiss, Z. Naturforsch. **48a,** 471 (1993).
[17] Further information on the crystal structure determination may be obtained from Fachinformationszentrum Karlsruhe, Gesellschaft für wissenschaftlich-technische Information mbH, D-7514 Eggenstein-Leopoldshafen 2, Germany. Inquiries should be accompanied by the depository number CSD-56946, the names of the authors and the full literature reference.